scientific reports

Check for updates

OPEN

Lipoic acid-plumbagin conjugate protects pancreatic beta cells against high glucose-induced toxicity

Parveen Abdulhaniff[1], Chitra Loganathan[2,3], Penislusshiyan Sakayanathan[2] & Palvannan Thayumanavan[1]✉

Pancreatic β cells that produce insulin play a significant role in maintaining glucose homeostasis. However, high glucose (HG) causes oxidative stress, which leads to pancreatic β cell dysfunction. The synthesis of lipoic acid (LA) and plumbagin (PLU) conjugate (LA-PLU) was done and characterized using (1H) NMR, (13C) NMR, LC–ESI–MS/MS, and UV–visible spectroscopy techniques. ADME analysis confirmed the drug-like properties of LA-PLU. The present study revealed the protective effect of LA-PLU conjugate against HG (25 mM)-induced oxidative stress on pancreatic β cells. Cell viability was performed on RIN-5F cells and found that LA-PLU exhibits non-toxic up to 91.23 ± 2.61% of cell viability at 12.5 µM concentration. At 12.5 µM, LA-PLU protected pancreatic β cells up to 73.45 ± 3.72% under HG conditions. LA-PLU showed a protective effect on RIN-5F cells against HG-induced DNA damage, followed by preserving mitochondrial membrane potential and decreasing reactive oxygen species formation. Further, LA-PLU showed an anti-apoptotic effect by increasing the Bcl-2 (B cell lymphoma-2) level and decreasing the apoptotic proteins [Bcl-2 associated x (Bax), and cleaved caspase-3). Hence, the overall study concludes that LA-PLU could act as a potent antioxidant that protects the RIN-5F cells under HG conditions, resulting in the maintenance of glucose homeostasis.

Keywords Glucotoxicity, Pancreas, Lipoic acid, Plumbagin, Apoptosis

Hyperglycemia is a main feature in the development of type 2 diabetes mellitus (T2DM)[1]. Glucotoxicity caused by chronic hyperglycemia leads to structural and functional damage such as reduced beta (β) cell mass and low levels of insulin secretion[2]. Also, high glucose (HG) alters the function of mitochondria by increasing the level of reactive oxygen species (ROS)[3], which lead to impaired mitochondrial membrane potential (MMP), modulation of apoptotic proteins such as B cell lymphoma-2 (Bcl-2), and Bcl-2 associated x(Bax) ultimately leading to pancreatic β cell death[4]. Many studies have reported that HG causes elevated levels of pro-apoptotic proteins (Bax, cleaved caspase-3) and reduces Bcl-2 expressions which leads to pancreatic β cell death[5,6]. Pancreatic β cells are prone to damage because of poor antioxidant gene expression and a poor DNA repair mechanism[7,8]. Hence, it is necessary to regulate the HG-induced oxidative stress and protect the function of mitochondria, which increases the chance of survival of pancreatic β cells.

Lipoic acid (LA, thioctic acid) is a heterocyclic compound that contains two sulphur atoms and a carboxylic acid group. LA belongs to the dithiolane family, mainly heterocyclic thiol fatty acid[9]. LA is a well-known intracellular non-enzymatic mitochondrial antioxidant that is also present in foods. It is recognized as a nutritive antioxidant in animal foods by the FDA[10]. LA possesses a broad spectrum of activities like anticancer[11], neuroprotective[12], hepatoprotective[13], geroprotective[9] and antidiabetic[14]. LA has low bioavailability, plasma instability, and a short half-life[15]. LA analogues with COOH group modifications showed better therapeutic applications and plasma stability than LA[16,17]. A previous study reported that 0.5 mM LA inhibits HG-induced apoptosis in hamster pancreatic HIT-T15 cells[18]. LA partly alleviated mitochondrial dysfunction in SH-SY5Y-MOCK cells and SH-SY5Y-APP cells[19]. Mitochondria in ageing rats are structurally and functionally impaired by excessive oxidative stress, and LA reverses this damage by amplifying key antioxidant mechanisms that protect mitochondria[20]. An 80-day course of oral LA supplementation (600 mg/day) alleviates sperm oxidative stress, DNA damage and

[1]Molecular Therapeutics Laboratory, Department of Biochemistry, Periyar University, Salem, Tamil Nadu, India. [2]Bioinnov Solutions LLP, Research and Development Centre, Salem, Tamil Nadu, India. [3]Department of Prosthodontics and Implantology, Saveetha Dental College and Hospital, Saveetha Institute of Medical And Technical Sciences (SIMATS), Chennai, Tamil Nadu, India. ✉email: pal2912@periyaruniversity.ac.in

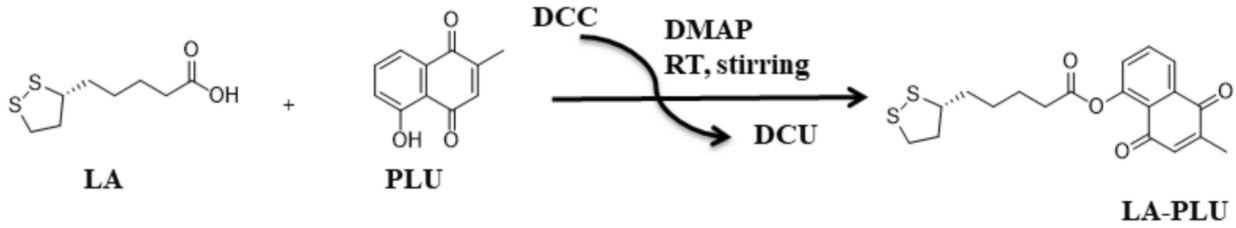

Fig. 1. Schematic representation of the synthesis of LA-PLU.

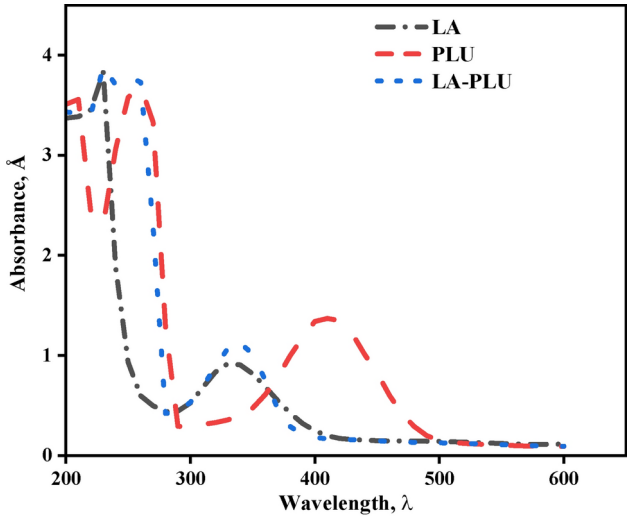

Fig. 2. UV–visible spectrum of LA, PLU and LA-PLU.

chromatin integrity in men with high sperm DNA damage[21]. LA–andrographolide conjugate ameliorates HG-induced oxidative stress damage in RIN-m cells[22].

Plumbagin (5-hydroxy-2-methyl-1,4-naphthoquinone, PLU), which is abundantly present in *Plumbago zeylanica* and belongs to the class of naphthoquinone heterocyclic compounds, possesses the following biological properties: anti-inflammatory[23], antimalarial[24], antifungal[25], antisterility[26], cardioprotective[27], anticancer[28], antidiabetic and wound healing[29]. PLU has challenges like limited solubility, bioavailability, and toxicity to be used as a drug. Therapeutic applications of PLU were widened by reducing its toxicity via esterification between the PLU 5-OH group and other phytochemicals like s-allyl cysteine[30,31]. PLU was reported to possess the ability to prevent HG-induced oxidative stress in the trophoblast cell line, HTR8/SVneo[32].

Keeping all these reports in view, the first in silico analysis of LA-PLU, ADME (Absorption, distribution, metabolism, and excretion) parameters was predicted using Schrodinger QiKprop tool. Then, novel LA-PLU conjugate was synthesized and characterized using UV–visible spectrophotometer, an electron spray ionization mass spectrometer (ESI–MS), and nuclear magnetic resonance (NMR) spectroscopy. Further, newly synthesized LA-PLU has been studied for its protective effect against HG-induced oxidative stress in RIN-5F cells. The protective efficacy of LA-PLU on cell viability, ROS formation, DNA damage, MMP, and the expression of apoptotic-related proteins like Bax, Bcl-2, and cleaved caspase-3 was studied.

Results

Synthesis and characterization of LA-PLU

LA and PLU were used as starting materials to proceed with the facile synthesis of LA-PLU using DCC in the presence of DMAP as a catalyst in the DCM solvent. Here, DCU is produced as a byproduct along with the heterocyclic LA-PLU conjugate (Fig. 1).

The UV–visible spectrum of LA-PLU is shown in Fig. 2. The λ max values for PLU were found to be 413 nm and 273 nm. The λ max for LA was determined to be 335 nm. The λ max values for LA-PLU were found to be 341 nm and 272 nm. The spectral data of LA-PLU in 1H NMR is δ (ppm): 2.08 (s, 3H, CH_3), 1.23–3.94 (m, 12H, CH_2), 3.97 (s, 1H, CH), 6.85–7.98 (m, 4H, ArH). 13C NMR is δ (ppm): 24.86 (CH3), 25.13–34.60 (CH_2), 49.97–56.52 (CH_2), 56.55 (CH), 123.46–149.2[33], 154.06 (Aliphatic C–O), 171.78 (Aliphatic C=O), 183.87 (ArC=O), 184.80 (ArC=O) (Fig. S1). The ESI mass spectrum for LA-PLU displayed a characteristic peak at m/z = 399 (Fig. S2). FTIR spectra of LA-PLU is given in Fig. 3. The peaks observed in FTIR spectra at 3288,2915, 2851, 1765, 1708, 1656, 1593, 1367, 1238, 1103, 1014, 919, 844, 776, 675, 405 cm^{-1} corresponds to Alkyne CH stretching, Asymmetric stretching of aliphatic CH_2 groups, Symmetric stretching of CH_2 groups, C=O stretching, Non

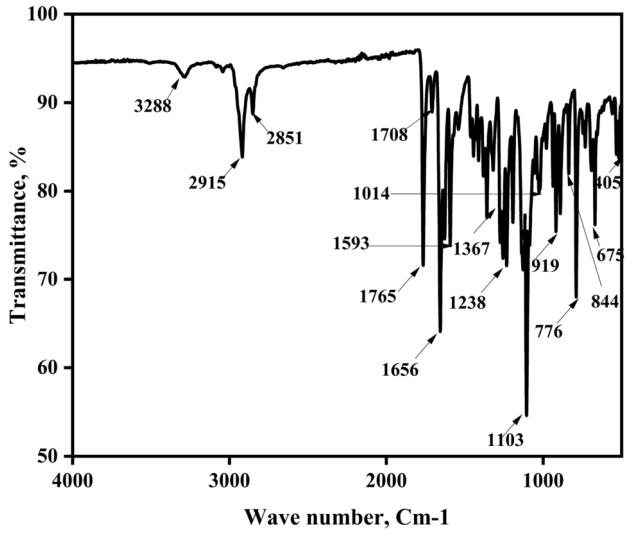

Fig. 3. FTIR spectrum of LA-PLU.

conjugated carbonyl stretching, Conjugated C=O group stretching, Aromatic C=C stretching, COO– symmetry stretching, C–O–C anti-symmetry stretching, C=S stretching, Carbon ring in cyclic compounds, Carbon ring in cyclic compounds, CH out of plane bending vibration, CH out of plane bending vibration, Aromatic ring bending vibrations, bromide.

The predicted ADME results of LA-PLU are presented in Table S1. Further, the radar plot is given in Fig. S3. From these results, it is understood that LA-PLU followed Lipinski's rule of five and pharmacokinetic parameters. The BOILED Egan's Egg plot determined that the LA-PLU may show good gastrointestinal absorption and less likely to cross the BBB (Fig. S3). The BOILED Egg plot white region represents the physiochemical space for good GI absorption and yolk represents the blood–brain barrier penetration. PGP-represents LA-PLU does not act as a substrate for P-glycoprotein efflux. The result obtained from prediction of activity spectra for substances (PASS) analysis of LA-PLU is given in Table S2. PASS predicts a list of targets and mechanisms of action of the LA-PLU. LA-PLU showed a high probability of acting as neuroprotectant, hepatoprotectant, antioxidant, antidiabetic, and anti-inflammatory agent.

Determination of LA-PLU on the cell viability of RIN5F cells

To understand the stability of LA-PLU in DMEM medium before treating the cells, the UV–visible spectrum of LA-PLU in DMEM was measured after 24 h. The UV–visible spectrum of LA-PLU was similar to λmax value of pure LA-PLU in DCM (Fig. S4). The retention of LA-PLU characteristic λmax values alongside unchanged spectral features after 24 h, confirms that LA-PLU is stable in DMEM for 24 h.

To determine the non-toxic concentration of PLU, LA and LA-PLU in the RIN-5F cell line, cells were treated with various concentrations of these compounds for 24 h. Cell viability was not affected up to 12.5 µM (91.23 + 2.16%) of LA-PLU. However, the cell viability was reduced at 25 µM of LA-PLU treatment (Fig. 4). Cell viability was affected in the presence of 6.25 µM PLU for 24 h. However, LA did not affect the cell viability up to 25 µM concentration (Fig. S5). Thus, the protective effect of LA-PLU against HG-induced toxicity was studied from a concentration of 1.5 to 12.5 µM. The protective effect of 3.125 µM of PLU and 12.5 µM of LA was also studied against HG-induced toxicity.

Determination of HG induced toxicity in the RIN-5F cell line.

To study HG induced toxicity in the RIN-5F cell line, the cells were treated with different glucose concentrations (12.5, 25, and 50 mM) for 24 h. Compared to control cells, HG concentrations showed toxicity for RIN-5F cells in a dose-dependent manner (Fig. 4). The cell viability was only 50% especially in the presence of 25 mM glucose. Hence, the protective effect of LA-PLU was studied against cells treated with a 25 mM HG concentration.

Protective effect of LA-PLU on RIN-5F under HG-induced toxicity

To investigate the protective effects of LA-PLU against HG-induced toxicity in the RIN-5F cell line, the cells were treated with PLU, LA, and LA-PLU for 2 h before HG administration and incubated along with respective compounds for another 24 h. LA-PLU has substantially safeguarded the survival of the RIN-5F cells against HG-induced toxicity in a dose-dependent manner. The representative figure of cells shows that at a 12.5 µM concentration of LA-PLU, the viability of cells was nearly 70% of the control level, reversing HG-induced toxicity. However, PLU did not protect the cells against HG-induced toxicity. LA at 12.5 µM concentration moderately protected the RIN-5F cells against HG-induced toxicity. These results show that the LA-PLU is superior to PLU, and LA individually in protecting the RIN-5F cells against HG-induced toxicity (Fig. 4).

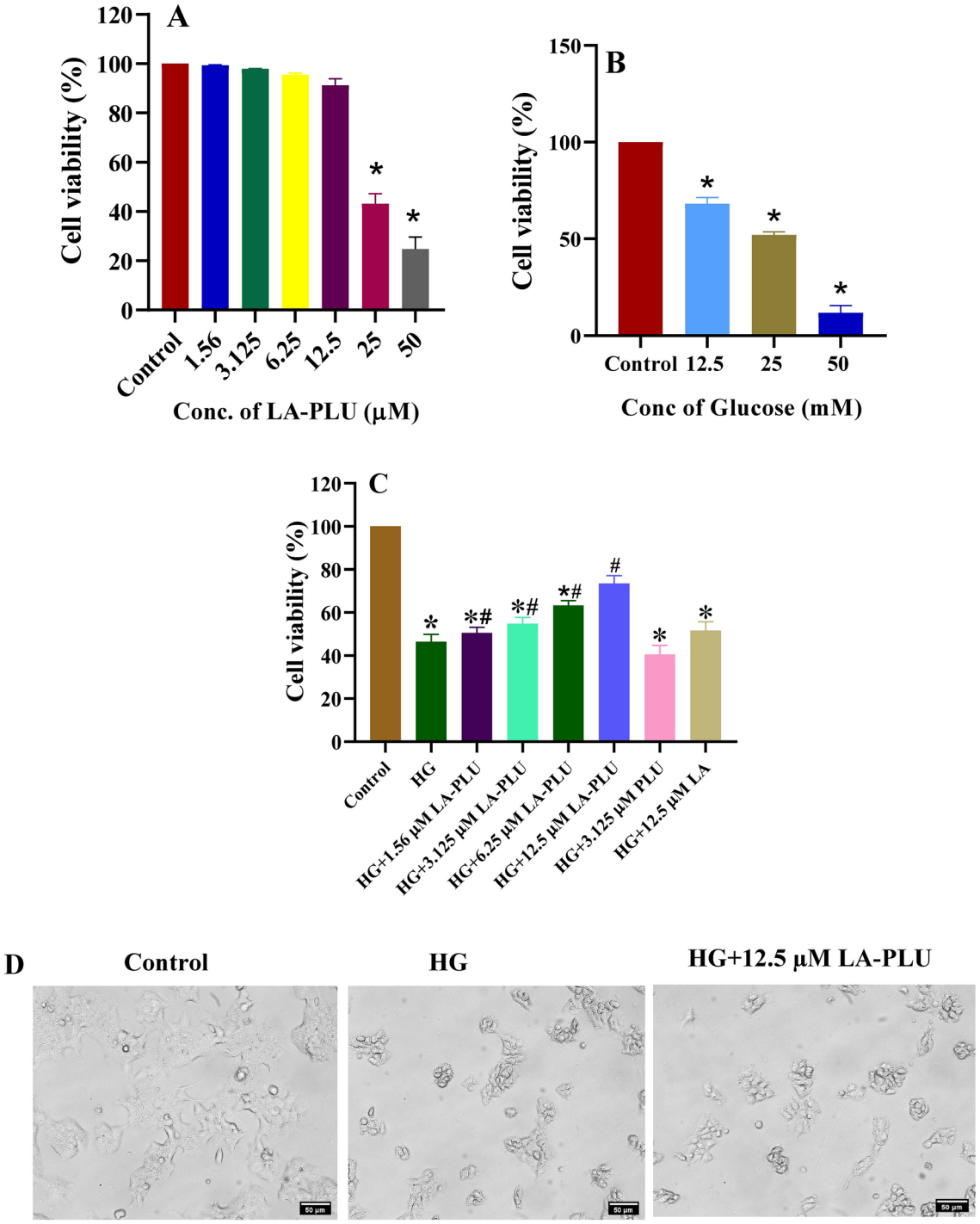

Fig. 4. Viability of RIN-5F cells under different conditions. (**A**) Effect of LA-PLU administration for 24 h in RIN-5F cells. (**B**) Effect of HG on RIN-5F cells. (**C**) Effect of PLU, LA, and LA-PLU on cell viability of RIN-5F cells cultured under HG (**D**) Representative figures show the RIN-5F cells from various groups. Viability is expressed as a percentage relative to the control group. n = 3; *$P < 0.05$ vs. control cells, #$P < 0.05$ vs. HG cells.

Detection of intracellular ROS generation using confocal microscopy

Exposure of RIN-5F cells to HG for 12 h triggered ROS generation, which was witnessed as raised green fluorescent intensity due to the oxidation of DCFH-DA by free radicals formed in comparison to control cells using a confocal microscope. However, LA-PLU treatment dose dependently hindered ROS generation, which was visualized as less green fluorescence. The relative fluorescent intensities measured using imageJ software are given in Fig. 5.

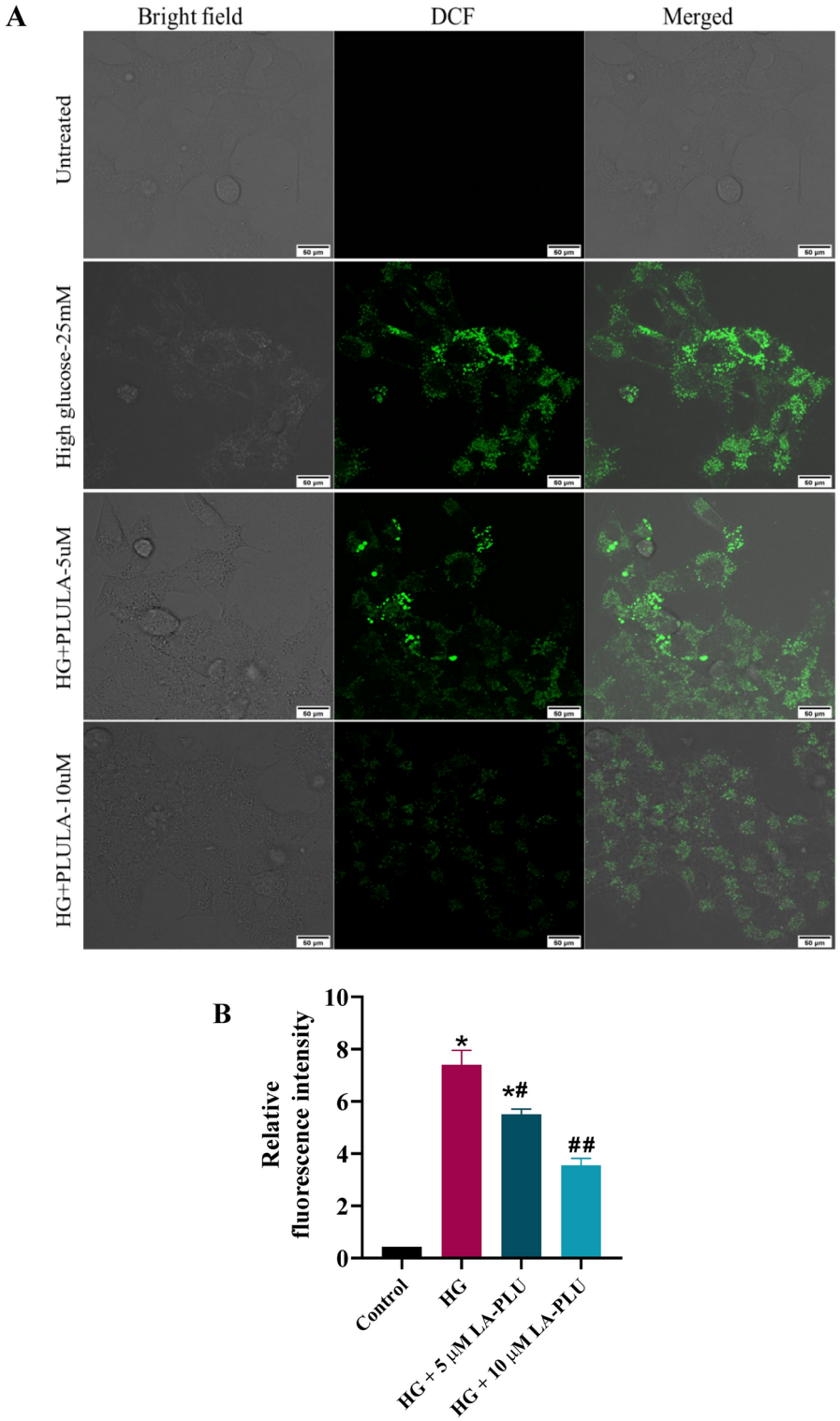

Fig. 5. Effect of LA-PLU against HG-induced oxidative stress in RIN-5F cells. (**A**) ROS generation in RIN-5F cells detected by DCF-DA in RIN-5F pancreatic beta cell lines cultured in HG and LA-PLU treated under HG (**B**) Corresponding quantitative analysis of the relative fluorescence intensity using imageJ software. Values are expressed as a percentage relative to the control group. n = 3; *$P < 0.05$ vs. control cells, #$P < 0.05$ vs. HG.

Effect of LA-PLU against HG-induced mitochondrial dysfunction in RIN-5F cells

The MMP investigation uses JC-1 dye. Active mitochondria fluoresce a brighter red signal, whereas mitochondria with lower MMP exhibit a green fluorescence signal. The level of depolarized mitochondria raised in HG-exposed cells, whereas LA-PLU protected mitochondrial damage in a dose-dependent manner. LA-PLU treatment has raised the MMP level significantly in HG-induced toxicity in RIN-5F cells (Fig. 6).

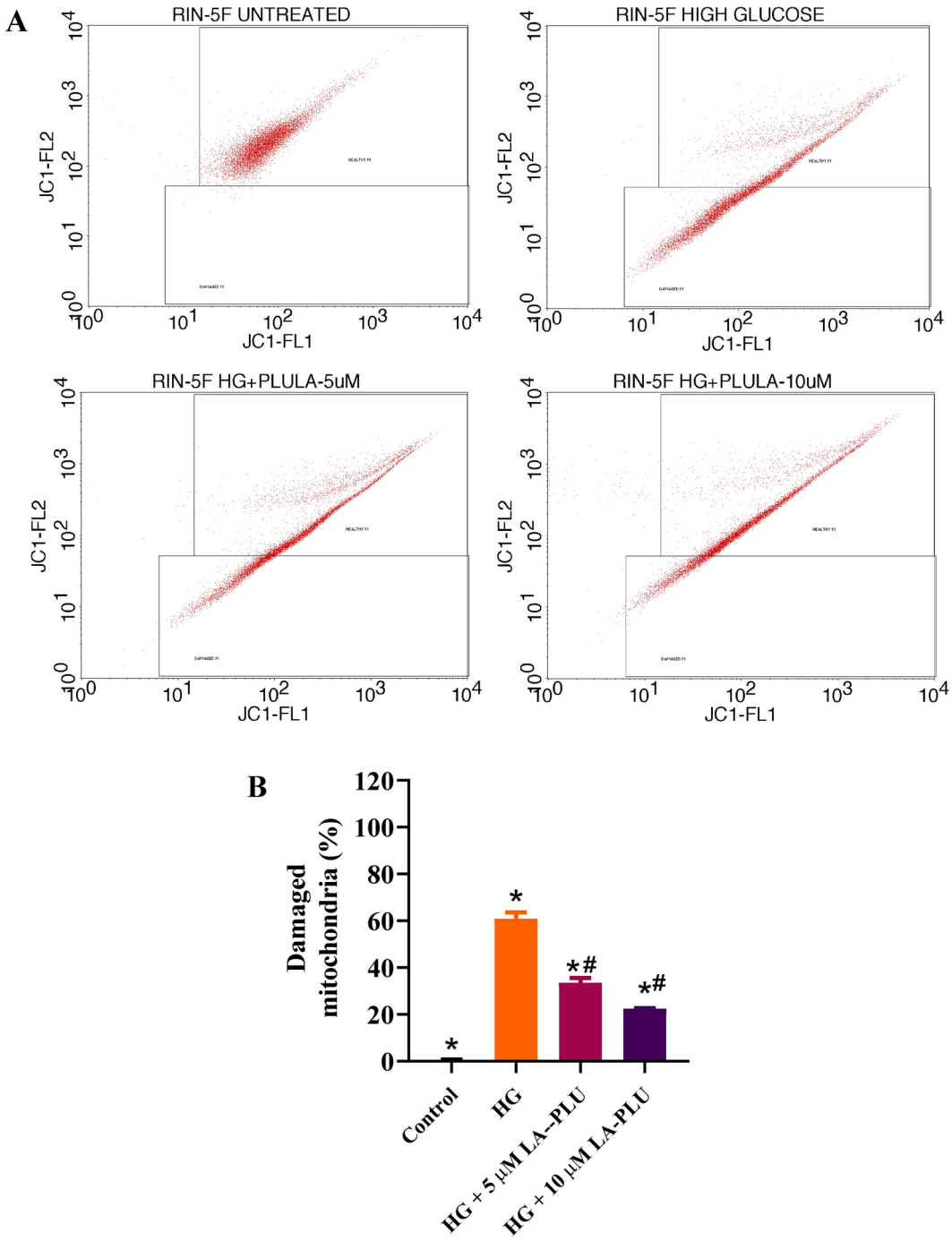

Fig. 6. Effect of LA-PLU against HG- induced mitochondrial dysfunction in RIN-5F cells. (**A**) Representative histogram obtained using flow Cytometry of the MMP assay from various groups is shown. (**B**) Corresponding percentage quantity of mitochondria present in various groups of cells. n = 3; *$P < 0.05$ vs. control cells, #$P < 0.05$ vs. HG.

Effect of LA-PLU against HG-induced DNA damage in RIN-5F cells

The fluorescent marker dUTP FTIC was used to label fragmented DNA. Quantitative measurement of DNA fragmentation was evaluated by a TUNEL assay using flow cytometry (Fig. 7). Treatment with LA-PLU has significantly reduced the DNA fragmentation in HG-induced RIN-5F cells.

Protective effect of LA-PLU against HG-induced apoptosis damage in RIN-5F cells

In apoptotic analysis, the number of live cells was reduced simultaneously with a significantly raised number of both early and late apoptosis by exposure of RIN-5F cells to HG. Control cells fluoresced uniformly with a green colour, which indicates that all cells are viable. However, in HG-induced RIN-5F cells, most of the cells had a granulated or cresent-shaped green nucleus (a condensed form of chromatin) due to AO staining, which was present on one side of the cells, indicating early apoptosis. In addition, cells in late apoptosis with concentrated and asymmetrically localized orange nuclear DNA due to EB staining were present. Treatment of HG-exposed RIN-5F cells with LA-PLU reduced the apoptotic morphology; in particular, at a 10 µM concentration of LA-

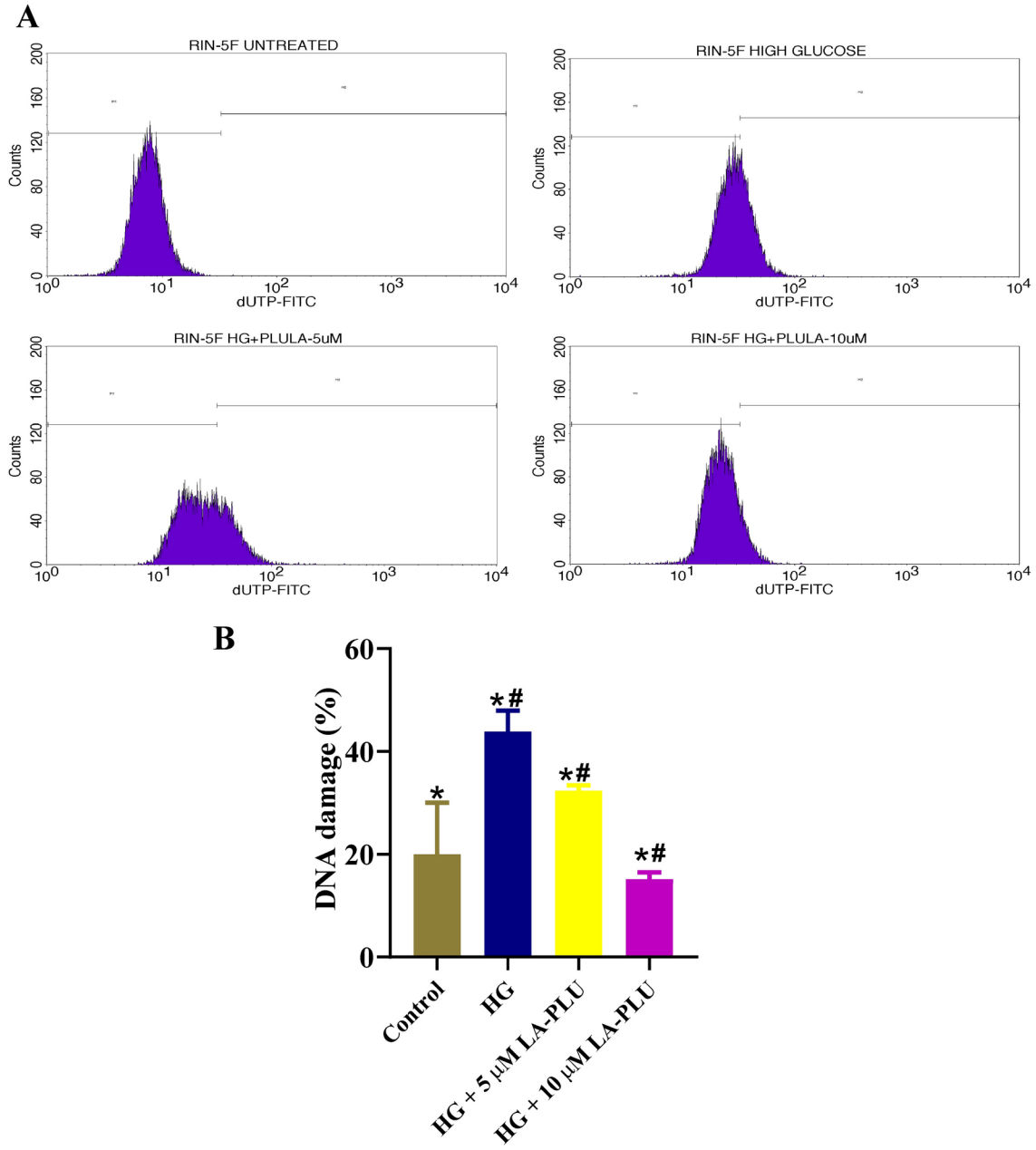

Fig. 7. Effect of LA-PLU against HG-induced DNA damage in RIN-5F cells. (**A**) Representative histogram obtained using flow Cytometry (**B**) Percentage of DNA damage from various groups of cells determined using TUNEL assay n = 3; *$P < 0.05$ vs. control cells, #$P < 0.05$ vs. HG cells.

PLU treatment, the cell morphology was similar to that of control cells. LA-PLU treatment raised the number of live cells significantly in HG-induced RIN-5F cells (Fig. 8).

Effect of LA-PLU against HG-induced expression of apoptotic markers

To explore the mechanism underlying the reduction of β cell apoptosis by LA-PLU in the present study, the involvement of pro- and anti-apoptotic proteins using flow cytometry was investigated. The representative overlay figures of flow cytometry analysis of the expression of proteins Bcl-2, Bax, and cleaved caspase-3 from various groups of RIN-5F cells are shown in Fig. S6. The level of Bax (proapoptotic protein) has raised, whereas the level of Bcl-2 (antiapoptotic protein) has reduced in HG-induced RIN-5F cells. LA-PLU treatment prevented the changes in Bax, and Bcl-2 quantities in HG-induced RIN-5F cells. Due to this, the level of cleaved caspase 3 raised under the HG condition and reduced under LA-PLU treatment in HG-induced RIN-5F cells (Fig. 9).

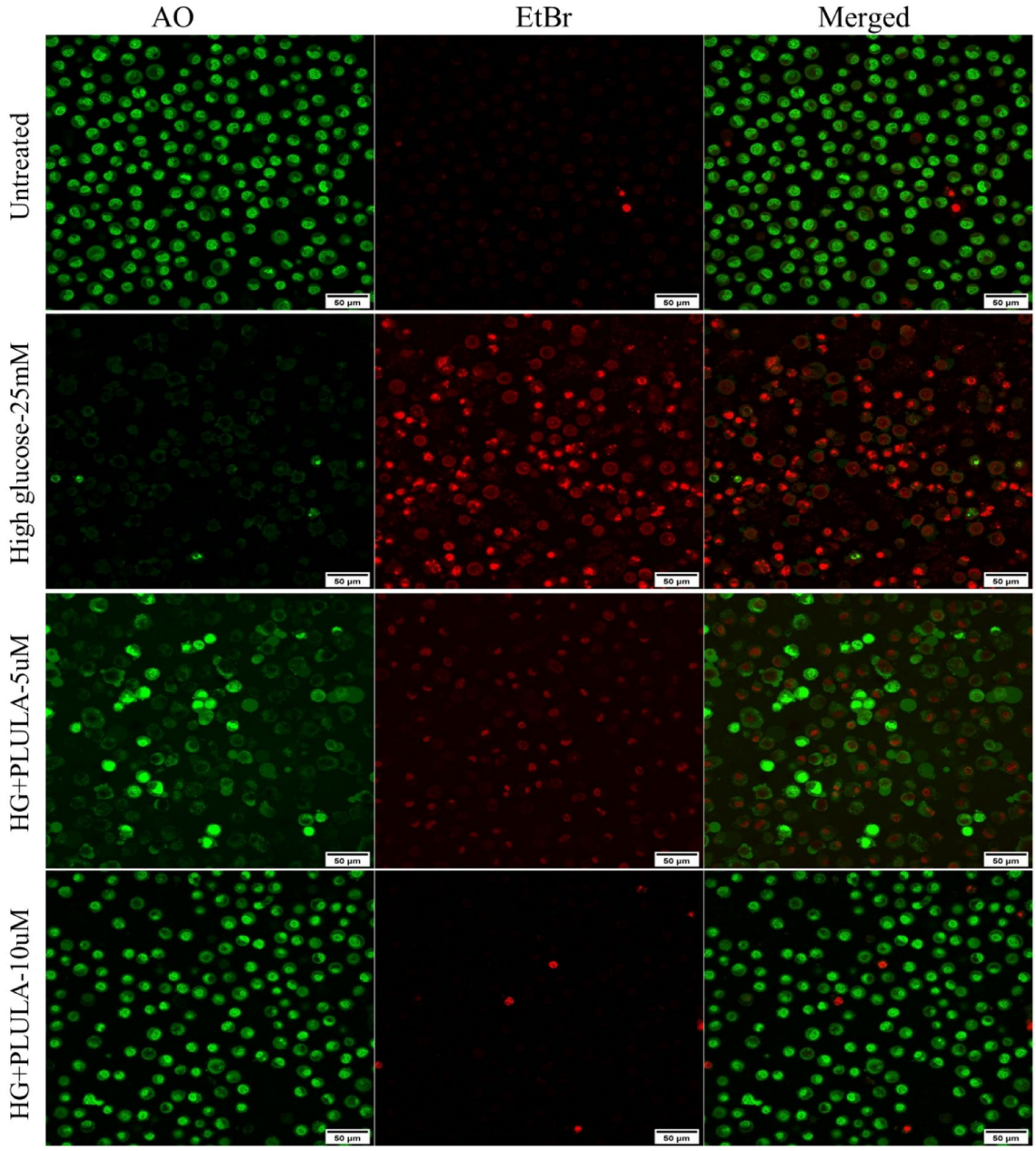

Fig. 8. Effect of LA-PLU on apoptosis under HG in RIN5F cells. Representative AO/EtBr-stained cell figures from various groups. Most of the cells were undergoing apoptosis in the HG group. However, LA-PLU treatment has preserved the cell viability as visualized by the increase in green fluorescence cells in HG groups.

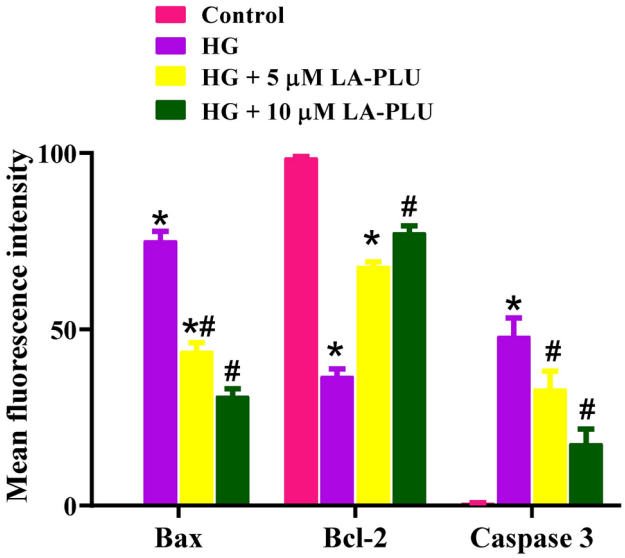

Fig. 9. Effect of LA-PLU against HG-induced alteration in expression of apoptosis-related proteins in RIN-5F cells. Mean fluorescence intensities of various proteins in RIN-5F cells from various groups. n = 3; *$P < 0.05$ vs. control cells, #$P < 0.05$ vs. HG cells.

Discussion

HG-induced oxidative stress in pancreatic β cells linked to the onset and progression of T2DM pathogenesis[34,35]. In recent years, LA conjugates have received considerable attention due to their improved biological and pharmacological properties such as anti-cancer[36], antimicrobial[37], anti-aging[37], antioxidant[38], α-amino-3-hydroxy-5-methyl-4-isoxazolepropionic acid receptor antagonist[39], anti-diabetic[40], neuroprotective[41] and cardioprotectant[42]. The LA-PLU synthesis was carried out and characterized thoroughly. ADME analysis, which predicts and enhances drug research and development, also confirmed the drug-like properties of LA-PLU[43,44]. The lipophilicity (LogP) of a pharmaceutical molecule is expressed by its partition coefficient in both organic and aqueous phases. The LogP value influences the rate at which the drug molecules are absorbed by the body, where a lower LogP value corresponds to higher absorption and vice versa. The high lipophilic nature of LA-PLU (-0.718) would be advantageous because it could readily cross the blood–brain barrier[45]. The permeability of LA-PLU to the biological barrier is influenced by the topological polar surface area and molecular weight. The drug molecule's higher permeability is correlated with a lower molecular weight (376) and vice versa[46]. Using SwissADME software, the positioning of LA-PLU in the BOILED-Egg plot helps to predict its pharmacokinetic properties, particularly gastrointestinal absorption and BBB layer penetration[47]. From the purely pharmacokinetic standpoint, LA-PLU radar plot showed improved bioavailability in terms of predictable systemic oral absorption which may be preferable when peripheral targeting is involved[48,49].

The current study has elucidated the protective function of LA-PLU against apoptosis produced by HG in pancreatic β cells. The LA-PLU treatment effectively maintained the survival of pancreatic β cells in the presence of HG-induced damage. LA-PLU therapy reduced the characteristic features of apoptosis, such as DNA damage and changes in the shape of apoptotic cells, in pancreatic β cells exposed to HG circumstances. The increase in ROS formation under HG conditions is reduced by treatment with LA-PLU. It would be an indispensable event in the protection of cell viability. It has been reported that HG-induced oxidative stress in pancreatic β cells is primarily driven by the raised ROS generation[50]. ROS has the ability to oxidize or nitrify proteins, lipids and DNA by direct chemical modification[51]. LA-PLU protected DNA from damage in µM concentration. There is myriad of reports showing the protective efficacy of conjugates against oxidative stress-induced DNA damage higher than parent phytochemicals[52,53].

A number of non-communicable diseases, such as cancer, obesity, and T2DM, have mitochondrial damage pointed out as an important trigger for pathogenesis development[54]. HG-induced oxidative stress leads to a reduced number of mitochondria, and changes in their morphology, like raised volume, surface area, size, and reduction of proteins in the mitochondrial membrane, are associated with impaired MMP[55]. The mitochondrial pathway is known to contribute to the initiation and development of the apoptotic process and occurs through caspase-3 activation, which ultimately results in apoptosis[56].

Bcl-2 family proteins are small globular proteins and evolutionarily conserved regulators of apoptosis[33]. Bcl-2 belongs to the Bcl-2 family that mediates the pro survival of cells. Bcl-2 has two different structures, an intact hydrophobic groove that is responsible for its antiapoptotic activity[57]. Generally, cellular redox status has been shown to play an important role in the activation and antiapoptotic function of Bcl-2[58]. Exposure of cells to HG induced oxidative stress leads to diminished expression of Bcl-2.

LA-PLU treatment prevented the abnormal increase of Bax protein in HG conditions in pancreatic β cells. Raised expression of Bax is associated with apoptosis in various cells such as pancreatic β cells, proximal tubule

epithelial cells, chondrocytes[59]. Bax is a cytosolic the proapoptotic in pancreatic β cells. In HG conditions, Bax activated, relocated, and formed pores with Bak on the mitochondrial outer membrane[60].

Cleaved caspase-3 activated through Bax was found to be reduced by Bcl-2. Hence, suppression of Bax and cleaved caspase-3 under HG conditions by LA-PLU treatment has further raised the protective efficacy of pancreatic β cells. ROS triggered MMP impairment emerged as a key event in the Bax mediated apoptosis, while protection of mitochondrial function and reduction of specific marker expression might appear jointly responsible for the protective effect of LA-PLU against HG-induced oxidative stress. Numerous studies explore the effect of HG on pancreatic β cell apoptosis and protecting mechanisms involving apoptotic markers (cleaved caspase-3), anti-apoptotic proteins (Bcl-2) and pro apoptotic proteins (Bax)[61–64]. Further, it suggests that LA-PLU may have inhibited HG induced β cell apoptosis by reducing the expression of Bax, cleaved caspase-3, pro-apoptotic proteins involved in cell death, and enhancing Bcl-2 expression.

Material and methods

Materials

The rat pancreatic cell line RIN-5F was procured from the National Centre for Cell Science, Pune, India. The MMP Detection and APO DIRECTTM kit for the TUNEL (Terminal Deoxynucleotide Transferase dUTP Nick End Labelling) analysis (Catalogue No. 551302) were purchased from BD Sciences, USA. Dulbecco Modified Eagle Medium (DMEM), 3(4, 5-dimethylthiazol-2-yl)-2,5-diphenyl tetrazolium (MTT), foetal bovine serum (FBS), sodium azide, bovine serum albumin (BSA), glucose, nitroblue tetrazolium (NBT), and D-phosphate buffered saline (PBS) solution were procured from Himedia, Pvt. Limited, Mumbai, India. LA and PLU were bought from Sigma, USA. The FITC-conjugated antibodies against the human proteins Bcl-2 (catalogue No. 556535) and cleaved caspase 3 (catalogue No. 559341) were acquired by BD Pharmingen (San Jose, CA, USA). FITC conjugated Bax antibody (catalogue No. 139543) was acquired from Abcam, Cambridge, MA, USA. The fluorescent dyes 2′, 7″ dichlorofluorescein diacetate (DCFH-DA), acridine orange (AO), and ethidium bromide[51] were acquired from Life Technologies, Invitrogen, and Carlsbad, CA, USA.

Methods

Synthesis of LA-PLU

LA-PLU is synthesized as explained earlier[31]. In short, 20 ml of DCM was used to solubilize a mixture of 10 mg PLU, 50 mg LA, 200 mg DCC, and 2 mg DMAP to esterify LA and PLU. The reaction mixture was stirred for 5 h at room temperature and rinsed twice with a 5% citric acid solution in order to remove DMAP and dicyclohexylurea (DCU) that were formed as byproducts. The LA-PLU was purified with silica gel (60–120 mesh) using column chromatography using a hexane to ethyl acetate ratio between 9:1 and 8:2.

Characterization of LA-PLU

The UV–visible spectrum of LA, PLU, and LA-PLU was obtained by scanning wavelengths from 300 to 600 nm using a UV–vis (UV-1800, Shimadzu, Kyoto, Japan). DMEM was used as a control and LA-PLU in DMEM was incubated for 24 h at 37 °C to investigate the stability of the LA-PLU in media, followed by a UV–visible spectrum that was obtained as suggested above. ESI–MS was obtained using the Waters Q-TOF micromass spectrometer. 1H-NMR and 13C-NMR spectra were measured at the frequency of 400 MHz at the hexadeutro-DMSO by an ultra-shield model Bruker spectrophotometer with an internal standard of tetramethylsilane. Fourier transform infrared spectroscopy (FTIR) was done to predict functional groups and confirm ester formation (Spectrum Two, Perkin Elmer, USA).

ADME analysis

The pharmacokinetic and pharmacodynamic properties of LA-PLU including molecular weight, the Lipinski rule, the octanol/water partition coefficient (logP) and GIT absorption were analyzed with QiKprop (Schrodinger release 2021-1). Biological radar, Egan's boiled egg model (SwissADME)[47] and prediction of activity spectra for substances (PASS, way2drug)[48,49].

Cell culture and treatment

The RIN-5F cell line was cultured at a temperature of 37 °C, 5% atmospheric CO2 in DMEM containing 5 mM glucose and 10% FBS. About 20,000 cells were seeded and allowed to grow for 24 h. The cells were then treated with different concentrations of glucose (12, 25 and 50 mM) for 24 h to determine HG-induced toxicity. To determine the toxicity of PLU, LA, and LA-PLU to RIN-5F cells, the cells were treated with different concentrations of compounds for 24 h. To understand the protective effect of PLU, LA, and LA-PLU against HG-induced toxicity, the cells were treated in the following groups: control group (untreated), HG group (25 mM of glucose), HG + LA-PLU group (cells treated with 5, 10 and 15 µM of LA-PLU for 2 h, after which 25 mM glucose were added and incubated together with LA-PLU for 24 h), HG + 3.125 µM of PLU, and HG + 12.5 µM of LA.

MTT assay

Cell viability was determined using MTT. In brief, at the end of treatment, the cells were incubated for 1 h in a 37 °C CO2 incubator in the presence of a solution of the MTT reagent (0.5 mg/ml in DMEM). After removing MTT, the color crystals were solubilized with 100 µl of DMSO and measured at 570 nm using a microplate spectrophotometer (ELX-800, Biotek, CA, USA).

Detection of ROS generation and apoptosis using confocal microscopy

The cells were incubated at a final concentration of 1 µM DCFH-DA in the medium for 30 min in a CO2 incubator under dark conditions to visualize intracellular ROS production. For the analysis of apoptosis, cells

were stained with 100 µg/ml of AO and 100 µg/ml of EB. Fluorescent figures were obtained with confocal laser scanning microscopy (Carl Zeiss LSM 880, Germany). Image J software was used to process the images.

Determination of LA-PLU protection against HG-induced mitochondrial dysfunction in RIN-5F cells
At the end of the treatment, the MMP was detected with MMP detection kit according to the manufacturer's instructions. (BD Biosciences, USA). Briefly, the cells were trypsinized and centrifuged at 300 × g at 25 °C to remove the medium. About 0.5 ml of working JC-1 solution was added to the cells, mixed well, and incubated in a CO2 incubator for 15 min. After the incubation period, the cells were washed with the 1X assay buffer provided in the kit. The cells were analyzed by flow cytometry using the FL1 and FL2 channels. (BD FACS Calibur, BD Biosciences, CA, USA).

Determination of DNA fragmentation using flow cytometry
At the end of the treatment, fixation of the RIN-5F cells was done using 70% ethanol. DNA fragmentation was carried out using the TUNEL assay kit according to the manufacturer's instructions. At the end of the staining, the cells were analyzed by flow cytometry (BD FACS Calibur, BD Biosciences, USA). The DNA fragmentation was detected using the FL-1 channel, recording the number of cells using green fluorescence at 515–555 nm.

Protein expression analysis using flow cytometry
After the completion of the treatment period, the cells were subjected to fixation and permeabilization using the BD cytofix/cytoperm solution. Then, the cells were washed with 0.5% BSA and 0.1% sodium azide containing 1X PBS, pH 7.2. About 20 µl of these antibodies were added and incubated for 30 min in the dark at 25 °C. The cells were washed again with 1X PBS (pH 7.2), which contains 0.1% sodium azide. The stained cells were analyzed by flow cytometry with excitation and emission wavelengths (λ) 494 and 520 nm for FITC (FL-1 channel), respectively. For PE, the wavelengths of excitation and emission used were 488 and 578 nm (FL-2 channel), respectively.

Statistical analysis
All experiments were performed in triplicates. All data were summarized as the means ± SD and analyzed using GraphPad Prism (GraphPad Software, San Diego, CA, USA). One-way analysis of variance (ANOVA) was applied to analyze data for comparisons between groups, followed by Tukey's multiple range tests for post-hoc analysis. $P < 0.05$ was considered significant.

Conclusion
HG is a hallmark feature of T2DM. LA-PLU was synthesized and characterized using UV–vis, NMR, and LC–MS. It's evident that LA-PLU is not toxic to RIN-5F cells up to 12.5 µM with normal cell morphology. LA-PLU improved cell viability and reduced MMP and ROS accumulation in RIN-5F cells against HG. It also protected against HG-induced apoptosis in RIN-5F cells, demonstrating its potential therapeutic value in the treatment of oxidative stress. LA-PLU modulates the expression of Bcl-2, Bax, and cleaved caspase-3 in the HG condition. Present research suggests that LA-PLU is a promising candidate for controlling the apoptosis mediators of pancreatic β cells and provides excellent protection against HG.

Data availability
Data will be provided by corresponding author on request.

Received: 9 July 2024; Accepted: 6 March 2025
Published online: 01 April 2025

References
1. Campbell, J. E. & Newgard, C. B. Mechanisms controlling pancreatic islet cell function in insulin secretion. *Nat. Rev. Mol. Cell Biol.* **22**, 142–158. https://doi.org/10.1038/s41580-020-00317-7 (2021).
2. Donath, M. Y. & Halban, P. A. Decreased beta-cell mass in diabetes: Significance, mechanisms and therapeutic implications. *Diabetologia* **47**, 581–589. https://doi.org/10.1007/s00125-004-1336-4 (2004).
3. Lanza, U. et al. Investigating the hypoglycaemic potential of processed apple and acarbose combination in vitro, ex vivo, and in vivo: the role of quercetin-3-glucoside in steering α-glucosidase inhibition. *Food Funct.* **16**, 1771–1780 (2025).
4. You, S., Zheng, J., Chen, Y. & Huang, H. Research progress on the mechanism of beta-cell apoptosis in type 2 diabetes mellitus. *Front. Endocrinol.* **13**, 976465 (2022).
5. Chang, C.-C. et al. Protective effect of *Siegesbeckia orientalis* on pancreatic β-cells under high glucose-induced glucotoxicity. *Appl. Sci.* **11**, 10963 (2021).
6. Dong, L. et al. A new labdane diterpenoid from *Scoparia dulcis* improving pancreatic function against islets cell apoptotic by Bax/Bcl-2/Caspase-3 pathway. *J. Ethnopharmacol.* **322**, 117571 (2024).
7. Guo, J. et al. Deciphering the molecular mechanism of Bu Yang Huan Wu decoction in interference with diabetic pulmonary fibrosis via regulating oxidative stress and lipid metabolism disorder. *J. Pharm. Biomed. Anal.* **243**, 116061 (2024).
8. Li, Q. et al. Osthole ameliorates early diabetic kidney damage by suppressing oxidative stress, inflammation and inhibiting TGF-β1/Smads signaling pathway. *Int. Immunopharmacol.* **133**, 112131 (2024).
9. Bethesda. https://pubchem.ncbi.nlm.nih.gov/compound/Thioctic-acid (National Center for Biotechnology Information, 2004).
10. Li, Z. et al. The effect of a-Lipoic acid (ALA) on oxidative stress, inflammation, and apoptosis in high glucose–induced human corneal epithelial cells. *Graefes Arch. Clin. Exp. Ophthalmol.* **261**, 735–748 (2023).
11. Mutlu, D., Seqme, M. & Arslan, Ş. Anticancer effects of alpha-lipoic acid on A172 and U373 human glioblastoma cells. *J. Inst. Sci. Technol.* **13**, 851–857 (2023).
12. Pei, X. et al. Neuroprotective effect of α-lipoic acid against Aβ25–35-induced damage in BV2 cells. *Molecules* **28**, 1168 (2023).
13. Al-Maathadi, A., Karawya, F., Al-Dalaen, S., Aljabali, A. & Satari, A. Alpha lipoic acid (ALA) alleviates hepatocytes toxicity of titanium dioxide nanoparticles in rats. *Indones. Biomed. J.* **15**, 231–239 (2023).

14. Dugbartey, G. J., Wonje, Q. L., Alornyo, K. K., Adams, I. & Diaba, D. E. Alpha-lipoic acid treatment improves adverse cardiac remodelling in the diabetic heart—The role of cardiac hydrogen sulfide-synthesizing enzymes. *Biochem. Pharmacol.* **203**, 115179. https://doi.org/10.1016/j.bcp.2022.115179 (2022).
15. Gruzman, A., Hidmi, A., Katzhendler, J., Haj-Yehie, A. & Sasson, S. Synthesis and characterization of new and potent α-lipoic acid derivatives. *Bioorg. Med. Chem.* **12**, 1183–1190. https://doi.org/10.1016/j.bmc.2003.11.025 (2004).
16. Kates, S. A., Casale, R. A., Baguisi, A. & Beeuwkes, R. III. Lipoic acid analogs with enhanced pharmacological activity. *J. Bioorg. Med. Chem.* **22**, 505–512 (2014).
17. Zhang, L. et al. Synthesis and biological activity of lipoic acid ester derivatives. *Gaodeng Xuexiao Huaxue Xuebao/Chemical Journal of Chinese Universities* **39**, 2198–2205. https://doi.org/10.7503/cjcu20180270 (2018).
18. Yang, Y. et al. α-lipoic acid inhibits high glucose-induced apoptosis in HIT-T 15 cells. *Dev. Growth Differ.* **54**, 557–565 (2012).
19. Hoffmann, L. F. et al. Neural regeneration research model to be explored: SH-SY5Y human neuroblastoma cells. *Neural Regen. Res.* **18**, 1265–1266. https://doi.org/10.4103/1673-5374.358621 (2023).
20. McCarty, M. F., Barroso-Aranda, J. & Contreras, F. The, "rejuvenatory" impact of lipoic acid on mitochondrial function in aging rats may reflect induction and activation of PPAR-gamma coactivator-1alpha. *Med. Hypotheses* **72**, 29–33. https://doi.org/10.1016/j.mehy.2008.07.043 (2009).
21. Habibi, M. et al. Alpha-lipoic acid ameliorates sperm DNA damage and chromatin integrity in men with high DNA damage: A triple blind randomized clinical trial. *Cell J.* **24**, 603–611. https://doi.org/10.22074/cellj.2022.8273 (2022).
22. Li, Y. et al. Andrographolide derivative AL-1 improves insulin resistance through down-regulation of NF-κB signalling pathway. *Br. J. Pharmacol.* **172**, 3151–3158. https://doi.org/10.1111/bph.13118 (2015).
23. Messeha, S. S. et al. The inhibitory effects of plumbagin on the NF-κB pathway and CCL2 release in racially different triple-negative breast cancer cells. *J. PLoS One* **13**, e0201116 (2018).
24. Gupta, A. C., Mohanty, S., Saxena, A., Maurya, A. K. & Bawankule, D. U. Plumbagin, a vitamin K3 analogue ameliorate malaria pathogenesis by inhibiting oxidative stress and inflammation. *Inflammopharmacology* **26**, 983–991. https://doi.org/10.1007/s10787-018-0465-1 (2018).
25. Dzoyem, J. P., Tangmouo, J. G., Lontsi, D., Etoa, F. X. & Lohoue, P. J. In Vitro antifungal activity of extract and plumbagin from the stem bark of *Diospyros crassiflora* Hiern (Ebenaceae). *Phytother. Res.* **21**, 671–674. https://doi.org/10.1002/ptr.2140 (2007).
26. Bhargava, S. K. Effects of plumbagin on reproductive function of male dog. *Indian J. Exp. Biol.* **22**, 153–156 (1984).
27. Li, Z., Chinnathambi, A., Ali Alharbi, S. & Yin, F. Plumbagin protects the myocardial damage by modulating the cardiac biomarkers, antioxidants, and apoptosis signaling in the doxorubicin-induced cardiotoxicity in rats. *Environ. Toxicol.* **35**, 1374–1385. https://doi.org/10.1002/tox.23002 (2020).
28. Liu, Y., Cai, Y., He, C., Chen, M. & Li, H. Anticancer properties and pharmaceutical applications of plumbagin: A review. *Am. J. Chin. Med.* **45**, 423–441. https://doi.org/10.1142/s0192415x17500264 (2017).
29. Shao, Y., Dang, M., Lin, Y. & Xue, F. Evaluation of wound healing activity of plumbagin in diabetic rats. *Life Sci.* **231**, 116422. https://doi.org/10.1016/j.lfs.2019.04.048 (2019).
30. Sagar, S. et al. Cytotoxicity and apoptosis induced by a plumbagin derivative in estrogen positive MCF-7 breast cancer cells. *Anti Cancer Agents Med. Chem.* **14**, 170–180 (2014).
31. Vijayan, S., Loganathan, C., Sakayanathan, P. & Thayumanavan, P. Synthesis and characterization of plumbagin S-Allyl cysteine ester: Determination of anticancer activity in silico and in vitro. *Appl. Biochem. Biotechnol.* **194**, 5827–5847 (2022).
32. Zhang, Y., Ni, G. & Yang, H. Plumbagin attenuates high glucose-induced trophoblast cell apoptosis and insulin resistance via activating AKT/mTOR pathway. *Qual. Assur. Saf. Crops Foods* **13**, 102–108 (2021).
33. Kopparapu, P. R. et al. Identification and characterization of a small molecule Bcl-2 functional converter. *Cancer Res. Commun.* **4**, 634–644. https://doi.org/10.1158/2767-9764.Crc-22-0526 (2024).
34. Strilbytska, O., Klishch, S., Storey, K. B., Koliada, A. & Lushchak, O. Intermittent fasting and longevity: From animal models to implication for humans. *Ageing Res. Rev.* **96**, 102274 (2024).
35. Sun, M., Chen, W.-M., Wu, S.-Y. & Zhang, J. Metformin in elderly type 2 diabetes mellitus: dose-dependent dementia risk reduction. *Brain* **147**, 1474–1482 (2024).
36. Yi, D., Yan, F. & Tian-Qin, C. Synthesis and anticancer activity of lipoic acid coumarin conjugate. *Nat. Prod. Res. Dev.* **32**, 379 (2020).
37. Lu, C. et al. Synthesis of lipoic acid–peptide conjugates and their effect on collagen and melanogenesis. *Eur. J. Med. Chem.* **69**, 449–454. https://doi.org/10.1016/j.ejmech.2013.09.011 (2013).
38. Xue, Z. et al. Synthesis of lipoic acid ferulate and evaluation of its ability to preserve fish oil from oxidation during accelerated storage. *Food Chem. X* **19**, 100802. https://doi.org/10.1016/j.fochx.2023.100802 (2023).
39. Qneibi, M., Nassar, S., Bdir, S. & Hidmi, A. α-lipoic acid derivatives as allosteric modulators for targeting AMPA-type glutamate receptors' gating modules. *Cells* **11**, 3608. https://doi.org/10.3390/cells11223608 (2022).
40. Zhang, Z. et al. Hypoglycemic and beta cell protective effects of andrographolide analogue for diabetes treatment. *J. Transl. Med.* **7**, 62. https://doi.org/10.1186/1479-5876-7-62 (2009).
41. Jalili-Baleh, L. et al. Chromone–lipoic acid conjugate: Neuroprotective agent having acceptable butyrylcholinesterase inhibition, antioxidant and copper-chelation activities. *DARU J. Pharm. Sci.* **29**, 23–38. https://doi.org/10.1007/s40199-020-00378-1 (2021).
42. Jayaraj, P. et al. A pre-formulation strategy for the liposome encapsulation of new thioctic acid conjugates for enhanced chemical stability and use as an efficient drug carrier for MPO-mediated atherosclerotic CVD treatment. *New J. Chem.* **44**, 2755–2767. https://doi.org/10.1039/C9NJ05258E (2020).
43. Hasan, Z., Safithri, M., Huda, A. & Kurniasih, R. In silico, to determine the active compounds of black tea and turmeric in increasing the activity of the enzyme sod. *Indones. J. Appl. Res. IJAR* **3**, 32–45. https://doi.org/10.30997/ijar.v3i1.187 (2022).
44. Prasanna, S. & Doerksen, R. J. Topological polar surface area: A useful descriptor in 2D-QSAR. *Curr. Med. Chem.* **16**, 21–41. https://doi.org/10.2174/092986709787002817 (2009).
45. Agbo, E. N., Gildenhuys, S., Choong, Y. S., Mphahlele, M. J. & More, G. K. Synthesis of furocoumarin–stilbene hybrids as potential multifunctional drugs against multiple biochemical targets associated with Alzheimer's disease. *Bioorg. Chem.* **101**, 103997. https://doi.org/10.1016/j.bioorg.2020.103997 (2020).
46. Alom, M. M. et al. Unveiling neuroprotective potential of spice plant-derived compounds against Alzheimer's disease: Insights from computational studies. *Int. J. Alzheimers Dis.* **2023**, 8877757. https://doi.org/10.1155/2023/8877757 (2023).
47. Dey, R. et al. Novel PLGA-encapsulated-nanopiperine promotes synergistic interaction of p53/PARP-1/Hsp90 axis to combat ALX-induced-hyperglycemia. *Sci. Rep.* **14**, 9483. https://doi.org/10.1038/s41598-024-60208-1 (2024).
48. Dey, R., Saha, S., Nandi, S., Molla, S. H. & Samadder, A. Exploring a new phyto-derived nanoparticle for targeting bacterial protein EF-Tu: An integrated approach to develop antimicrobial drug. *Smart Sci.* **12**, 357–372. https://doi.org/10.1080/23080477.2024.2338649 (2024).
49. Parasuraman, S. Prediction of activity spectra for substances. *J. Pharmacol. Pharmacother.* **2**, 52–53. https://doi.org/10.4103/0976-500x.77119 (2011).
50. Zhang, Z. et al. The cytotoxic role of intermittent high glucose on apoptosis and cell viability in pancreatic beta cells. *J. Diabetes Res.* **2014**, 712781. https://doi.org/10.1155/2014/712781 (2014).
51. Baines, C. P. et al. Loss of cyclophilin D reveals a critical role for mitochondrial permeability transition in cell death. *Nature* **434**, 658–662. https://doi.org/10.1038/nature03434 (2005).

52. Gerogianni, P. S., Chatziathanasiadou, M. V., Diamantis, D. A., Tzakos, A. G. & Galaris, D. Lipophilic ester and amide derivatives of rosmarinic acid protect cells against H_2O_2-induced DNA damage and apoptosis: The potential role of intracellular accumulation and labile iron chelation. *Redox Biol.* **15**, 548–556. https://doi.org/10.1016/j.redox.2018.01.014 (2018).
53. Shao, B. et al. Caffeic Acid Phenyl Ester (CAPE) protects against iron-mediated cellular DNA damage through its strong iron-binding ability and high lipophilicity. *Antioxidants* **10**, 798 (2021).
54. Zheng, Y. et al. A mitochondrial perspective on noncommunicable diseases. *Biomedicines* **11**, 647 (2023).
55. Kupsal, K. et al. Glucotoxicity and lipotoxicity induced beta-cell apoptosis in type 2 diabetes mellitus. *Int. J. Anal. Bio Sci.* **3** (2015).
56. Singh, N. et al. Chitosan/alginate nanogel potentiate berberine uptake and enhance oxidative stress mediated apoptotic cell death in HepG2 cells. *Int. J. Biol. Macromol.* **257**, 128717. https://doi.org/10.1016/j.ijbiomac.2023.128717 (2024).
57. Niu, G. et al. In *International Review of Cell and Molecular Biology* Vol. 313 (ed. Jeon, K. W.) 219–258 (Academic Press, 2014).
58. Qian, S. et al. The role of BCL-2 family proteins in regulating apoptosis and cancer therapy. *Front. Oncol.* **12**, 985363. https://doi.org/10.3389/fonc.2022.985363 (2022).
59. Wang, B. et al. High glucose suppresses autophagy through the AMPK pathway while it induces autophagy via oxidative stress in chondrocytes. *Cell Death Dis.* **12**, 506. https://doi.org/10.1038/s41419-021-03791-9 (2021).
60. Lopez, A. et al. Co-targeting of BAX and BCL-XL proteins broadly overcomes resistance to apoptosis in cancer. *Nat. Commun.* **13**, 1199. https://doi.org/10.1038/s41467-022-28741-7 (2022).
61. Choi, K. H., Park, M. H., Lee, H. A. & Han, J. S. Cyanidin-3-rutinoside protects INS-1 pancreatic β cells against high glucose-induced glucotoxicity by apoptosis. *Z. Naturforschung C* **73**, 281–289. https://doi.org/10.1515/znc-2017-0172 (2018).
62. Liu, L. et al. Dracorhodin perchlorate protects pancreatic β-cells against glucotoxicity- or lipotoxicity-induced dysfunction and apoptosis in vitro and in vivo. *FEBS J.* **286**, 3718–3736. https://doi.org/10.1111/febs.15020 (2019).
63. Park, S. Y. et al. Silk fibroin promotes the regeneration of pancreatic β-cells in the C57BL/KsJ-Lepr(db/db) mouse. *Molecules* **25**, 3259. https://doi.org/10.3390/molecules25143259 (2020).
64. Saddam, M. et al. Emerging biomarkers and potential therapeutics of the BCL-2 protein family: The apoptotic and anti-apoptotic context. *Egypt. J. Med. Hum. Genet.* **25**, 12 (2024).

Acknowledgements

Mrs. A. Parveen acknowledges Periyar University for providing a University Research Fellowship to carry out this research work (ref. No. PU/AD/AD-3/URF/03939/2021, dated March 10, 2021) and is also grateful to Bio-innov Solutions LLP, Research and Development Centre, Salem, Tamil Nadu for providing a lab facility to carry out this research.

Author contributions

P.A.: conceptualization, investigation, methodology, and writing-original draft; C.L.: conceptualization, writing-review, and editing; P.S.: Methodology, writing review, and editing; P.T.: conceptualization, supervision, writing- review, and editing.

Declarations

Competing interests

The authors declare no competing interests.

Additional information

Supplementary Information The online version contains supplementary material available at https://doi.org/10.1038/s41598-025-93344-3.

Correspondence and requests for materials should be addressed to P.T.

Reprints and permissions information is available at www.nature.com/reprints.

Publisher's note Springer Nature remains neutral with regard to jurisdictional claims in published maps and institutional affiliations.